Original Research

Degradation of Amido Black Dye Using Ultra-Violet Light Catalyzed by Iron Oxide Nanoparticles: Kinetics and Mechanism of Degradation

Olushola S. Ayanda [*], Cecilia C. Oforkansi, Omolola H. Aremu, Oluwakemi E. Ogunjemiluyi, Ololade L. Olowoyeye, Cecilia O. Akintayo

Nanoscience Research Unit, Department of Industrial Chemistry, Federal University Oye Ekiti, P.M.B 373, Oye Ekiti, Ekiti State, Nigeria; E-Mails: osayanda@gmail.com; olushola.ayanda@fuoye.edu.ng; oforkansicecilia@gmail.com; hellenlol@yahoo.com; omotokeoluwakemisola@yahoo.com; olowoyeyeololadelinda@gmail.com; cecilia.akintayo@fuoye.edu.ng

* **Correspondence:** Olushola S. Ayanda; E-Mails: osayanda@gmail.com; olushola.ayanda@fuoye.edu.ng

Abstract

In this study, we investigated the degradation of amido black dye in an aqueous solution using ultra-violet (UV) light catalyzed by iron oxide nanoparticles (nano-Fe). The nano-Fe was synthesized by sodium borohydride reduction of ferric chloride solution and was characterized by scanning electron microscopy (SEM), X-ray diffraction (XRD), and X-ray fluorescence spectrophotometry (XRF). The SEM of the nano-Fe showed regular spherical particles, the XRD examination showed a weak and broad peak at Fe (1 1 0), and the XRF study showed that the element with the highest composition was Fe_2O_3 (60.80%). The degradation experiments showed that the UV light catalyzed by nano-Fe could effectively degrade amido black dye. The nano-Fe/UV system could degrade 5 mg/L of amido black dye up to 93.2% at 254 nm after being irradiated for 60 min. The nano-Fe/UV system could be described by the Langmuir–Hinshelwood kinetic model, and the rate constants (k_{app}) were 0.0183–0.0323 min^{-1}. Thus, UV light combined with nano-Fe can be applied for the efficient remediation of dye wastewater.

1. Introduction

Water is indispensable for life. However, the quality of water is threatened by natural and anthropogenic activities. Wastewater containing inorganic and organic pollutants is predominately discharged from domestic, industrial, and public facilities and has deteriorated water quality in many parts of the world. Agricultural activities and manufacturing, mining, and processing industries release heavy metal ions, organic compounds, dyes, and other toxic pollutants regularly, thus contaminating groundwater and surface water [1]. Polluted water is unsafe for the ecosystem and human consumption. For example, dyes are extensively used in the textile industry and are also commonly used in the food, pharmaceutical, biological imaging, leather, plastic, liquid crystal, and cosmetic industries. There are greater than 10,000 different commercial dyes and pigments. Over 7×10^5 tons are produced annually worldwide [2] and around 5–10% of these dyes are discharged into the water as wastes [3]. Based on the structure, dyes can be classified into azo, diazo, acidic, basic, metal complex, etc. Additionally, dyes are commonly classified based on their source of production into natural dyes and synthetic dyes. Synthetic dyes resist decomposition due to their aromatic structures, which increase their physicochemical, thermal, and optical stability [4]. The azo-based dyes are the largest class of dyes; up to 60–70% of industrially synthesized dyes are azo compounds [5]. Color imparted by dyes is the first contaminant to be detected in water and must be removed from wastewater before it is discharged into water bodies [6]. Industrial wastewater containing dyes and their intermediates is usually toxic and carcinogenic to aquatic life. It causes serious environmental and aesthetic problems and reduces light penetration in water, which affects photosynthesis adversely [7]. Hence, dye effluents need to be treated before they are discharged into water bodies [8].

Various treatment techniques, such as adsorption, oxidation, coagulation/flocculation, ion exchange, photocatalysis, ozonation, electrochemical method, biological treatment, etc. [9], are used to remove dyes from contaminated water and wastewater. The treatment method to be applied depends on factors such as the organic or inorganic content, the concentration of the pollutant, toxicity, and environmental discharge standards [10]. Nanomaterials also play an important role in water treatment. Advanced materials developed through nanoscience and nanotechnology can effectively remove toxic pollutants from water and wastewater [11, 12]. In photocatalysis, iron is among the most used transition metal for catalyzing wastewater treatment [13]. Iron oxide is popular for catalysis due to its unique properties, such as excellent magnetic properties, extremely small size, high surface area-to-volume ratio, great biocompatibility, and surface modifiability [14]. According to many studies [1, 10, 15, 16], the use of iron for water purification has several advantages in the presence of ultra-violet (UV) light, visible light, and in the absence of light.

Iron oxide nanoparticles (nano-Fe) were synthesized for the photocatalytic degradation of methyl orange dye by Radini et al. [15]. The authors reported that the synthesized nano-Fe effectively degraded methyl orange dye under UV light. The degradation followed the pseudo-first-

order kinetics, and the rate constant k_{app} was 0.025 min^{-1}. Bishnoi et al. [16] synthesized magnetic nano-Fe using inedible *Cynometra ramiflora* fruit extract waste. The photocatalytic ability of the nano-Fe was investigated by the degradation of methylene blue dye under sunlight irradiation. The nanoparticles played a vital role in the environmental catalytic remediation of polluted water. Bibi et al. [17] investigated the green synthesis of nano-Fe using pomegranate seed extract and evaluated its photocatalytic activity for the degradation of textile dye. The authors reported that the synthesized Fe_2O_3 nanoparticles showed excellent photocatalytic activity against reactive blue under UV light irradiation, and the maximum degradation of 95.08% was achieved by conducting the reaction for 56 min. Meneceur et al. [18] investigated the photocatalytic activity of nano-Fe from plant extracts for degrading the diazo dyes Evans blue and Congo red. The nanoparticles that they produced were promising for application in water treatment technologies due to the simplicity of the synthetic technique and the possibility of inexpensive catalysis. Additionally, the synthesis of Fe_3O_4 nanoparticles derived from the sol-gel process (Facile, gram-scale, and tunable synthesis of Fe_3O_4, α-Fe_2O_3, and γ-Fe_2O_3 phases) was reported by Prakash et al. [19]. The photocatalytic efficiencies of the samples followed the order Fe_3O_4 > γ-Fe_2O_3 > α-Fe_2O_3 with 98, 87, 79/73% degradation of rhodamine B dye after 3 h. According to the authors, the photocatalytic recycle studies demonstrated that all synthesized photocatalysts showed excellent chemical stability and photo-stability.

In this study, the photocatalytic degradation efficiency of a model aqueous solution of amido black dye, particularly the kinetics and mechanism of degradation, was investigated. The effects of UV light, the amido black dye concentration, and irradiation time were considered.

2. Materials and Methods

2.1 Materials and Reagents

The amido black dye (Figure 1), ferric chloride ($FeCl_3 \cdot 6H_2O$), and sodium borohydride ($NaBH_4$) used in this study were procured from Sigma-Aldrich. A stock solution of 1,000 mg/L amido black dye was prepared in 1 L volumetric flasks. The working standard solutions were prepared from the stock solution by serial dilution.
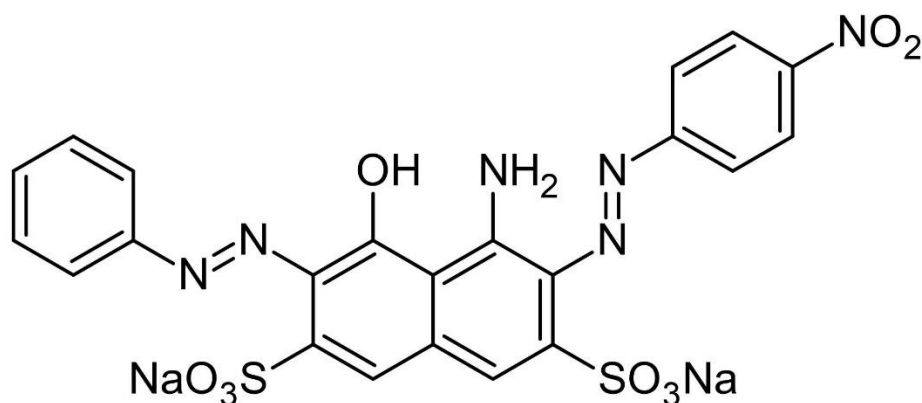

Figure 1 Amido black 10B.

Several techniques, such as scanning electron microscopy SEM (JOEL-JSM 7600F), X-ray fluorescence spectrophotometry (Phillips-JEE 4B), and X-ray diffraction analysis (BRUKER AXS, D8

Advance), were used to determine the specifications of the synthesized nano-Fe. Photocatalysis was conducted using an Analytikjena UV lamp (UVP UVGL-15; 4 Watt, 230V-50/60Hz).

2.2 Synthesis of Iron Oxide Nanoparticles

The synthesis of nano-Fe is shown in Equation 1. Initially, 27 mL of 0.2 M $FeCl_3 \cdot 6H_2O$ was transferred into a 500 mL three-neck round bottom flask and titrated with 50 mL of 0.2 M $NaBH_4$ solution. The solution was stirred vigorously with a stirring rod until the $NaBH_4$ solution was completely added to the ferric chloride solution [20]. The suspended black nano-Fe was filtered with Whatman No. 32 filter paper and dried in an oven at 100°C for 24 h.

$$Fe(H_2O)_6^{3+} + 3\,BH_4^- + 3H_2O \rightarrow Fe^0 + 3B(OH)_3 + 10.5H_2 \tag{1}$$
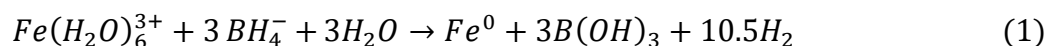
2.3 Degradation of Amido Black Dye

The amido black dye was degraded in the dark under UV light irradiation in a beaker with the nano-Fe catalyst. Then, 0.02 g of the nano-Fe was added to 50 mL of 5.0 mg/L solution of amido black dye. The UV lamp was placed above the beaker containing the solution, and the distance between the UV lamp and the amido black dye solution was about 14 cm. The samples were filtered after the time elapsed (10 - 60 min), and the absorbance of the degraded dye was measured at 619 nm using a Thermo Scientific UV/visible spectrophotometer (Model: Helios Epsilon 3SGM 320011). The degradation efficiency (%) was obtained using Equation 2. The effects of short and long UV wavelengths (254 and 365 nm), amido black dye concentration, and irradiation time on the degradation of the dye were investigated.

$$\% \, Degradation = \frac{AB_o - AB_t}{AB_o} \times 100 \tag{2}$$

Here, AB_o and AB_t denote the initial and final concentrations of amido black dye, respectively.

3. Results and Discussion

3.1 Characterization of Iron Oxide Nanoparticles

The SEM of the nano-Fe (at 8,000× magnification) showed regular spherical particles that were connected to each other(Figure 1). The X-ray diffractogram (Figure 2 and Figure 3) showed a weak and broad peak at Fe (1 1 0); the weak peak of the nano-Fe showed that the iron was reduced [21] and had a poor crystalline structure. XRF analysis of the nano-Fe showed that Fe_2O_3 was the most prevalent compound (60.80%) and the main element of the iron nanoparticles. The other prevalent compounds included SiO_2 (29.50 wt%) and Al_2O_3 (2.16 wt%), while TiO_2, CaO, P_2O_5, K_2O, MnO, MgO, and Na_2O were less prevalent, and their abundance ranged from 0.02–0.7 wt%.
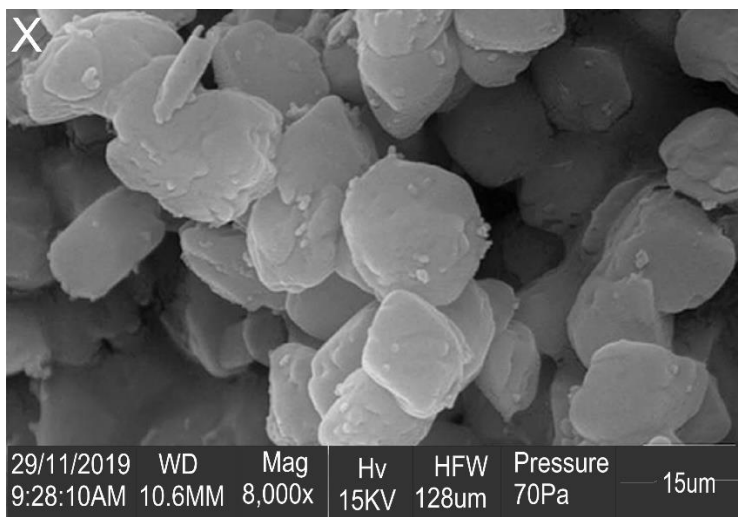
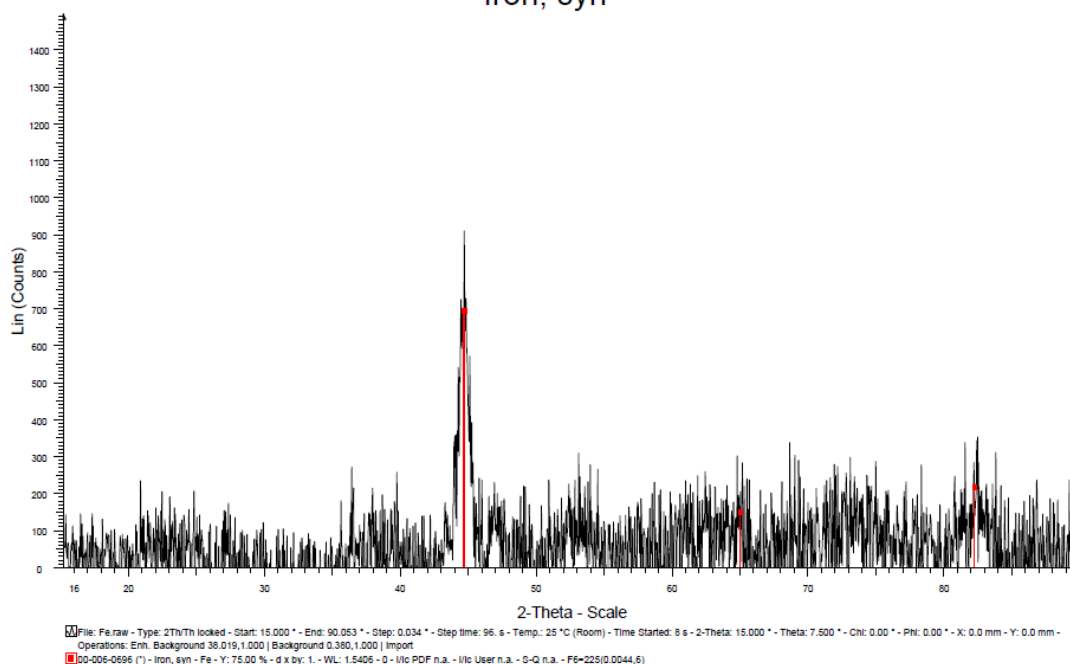**Figure 2** The scanning electron micrograph of nano-Fe.

Figure 3 The X-ray diffractogram of nano-Fe.

3.2 Photocatalytic Degradation

The photocatalysis of amido black dye caused a rapid increase in the degradation of amido black dye from 70.4% (10 min) to 91.2% (40 min) and 43.3% (10 min) to 65.4% (40 min) at 254 nm and 365 nm (UV wavelengths), respectively. The maximum degradation efficiencies of 93.2% and 68.8% at 254 nm and 365 nm, respectively, were obtained after 40 min (Figure 4).
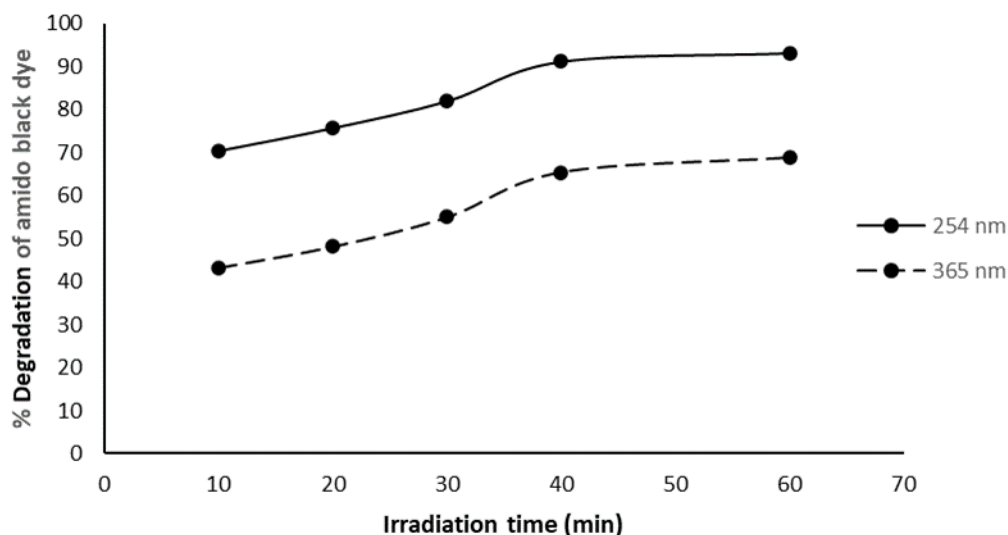
Figure 4 The effect of the irradiation time and the wavelength of UV light on the photocatalytic degradation of amido black dye.

By assuming pseudo-first-order reaction kinetics, Equation 3 was used to deduce the photocatalytic rate constants.

$$-\frac{dAB}{dt} = kAB \leftrightarrow ln\left(\frac{AB_o}{AB_t}\right) = kt \qquad (3)$$

Here, AB_o and AB_t denote the amido black dye concentrations at time 0 and t, respectively, and k denotes the pseudo-first-order rate constant (Figure 5).
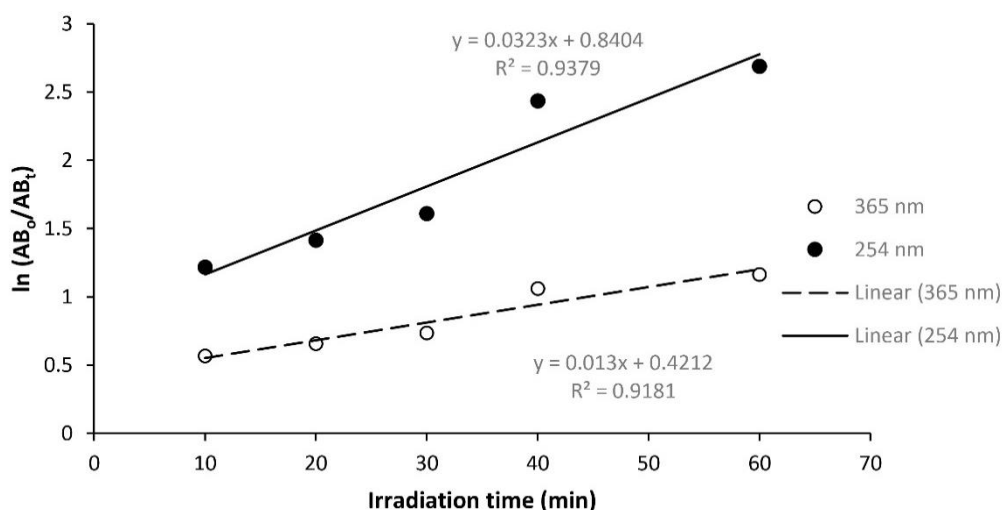

Figure 5 The kinetic plot of amido black dye photocatalytic degradation.

The rate constants for amido black dye photocatalytic degradation by UV irradiation in the presence of the nano-Fe catalyst at 254 and 365 nm were 0.0323 min^{-1} and 0.0130 min^{-1}, respectively. This showed that the photocatalytic degradation at 254 nm was about 2.5 times faster than that at 365 nm.

3.3 Mechanism of Degradation

The degradation of amido black dye by UV light catalyzed by nano-Fe followed the pseudo-first-order kinetics and depended on the concentration of amido black dye in the bulk solution (Equation 4).

$$r = -\frac{dAB}{d_t} = k_{app}t \qquad (4)$$

The integration of Equation 4 leads to Equation 5 (with $AB = AB_o$ at $t = 0$; AB_o denotes the initial concentration in the bulk solution and t denotes the reaction time); k_{app} denotes the apparent pseudo-first-order rate constant and was obtained from the slope of the plot of $ln\,{^{AB_o}/_{AB_t}}$ versus time (t) (Figure 6).

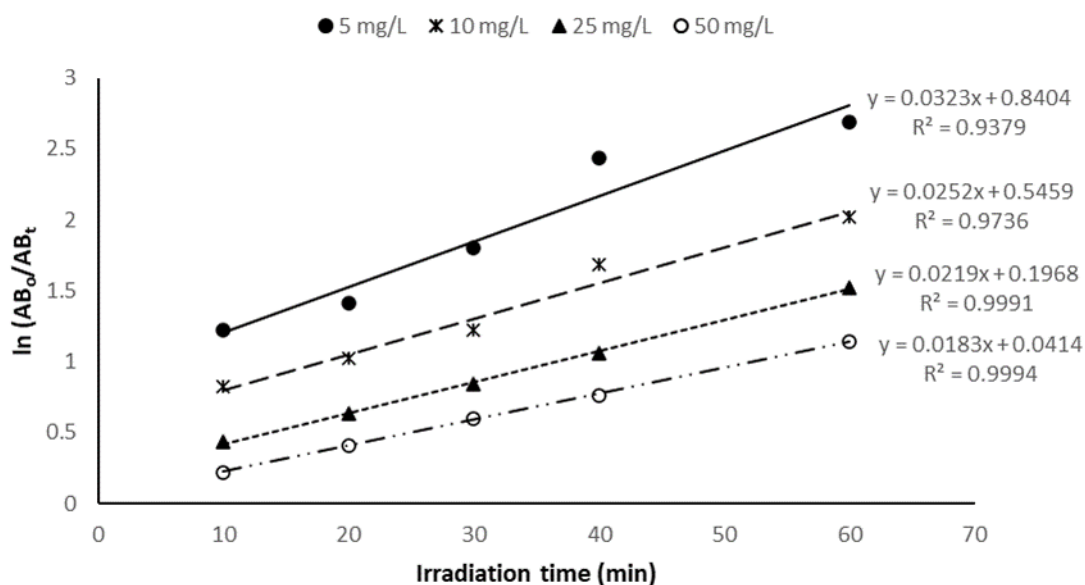$$ln\left(\frac{AB_o}{AB_t}\right) = k_{app}t \qquad (5)$$

Figure 6 The plot of *ln AB_o/AB_t* vs. time.

The degradation of amido black dye was well-fitted to a pseudo-first-order rate (Figure 6 and Table 1), i.e., the value of R^2 ranged from 0.9379 to 0.9994. The results of the experiments also indicated that the apparent pseudo-first-order degradation rate constant (k_{app}) of amido black dye decreased with an increase in the amido black dye concentration. The value of k_{app} evaluated in this study was similar to that obtained by Radini et al. [15].

Table 1 The apparent pseudo-first-order rate constants (k_{app}), R^2, and Langmuir–Hinshelwood model constants.

Amido black dye	UV light catalyzed by nano-Fe			K_{LH}	kc
(mg/L)	Rate Equations	k_{app} (min^{-1})	R^2	(L/mg)	(mg/L/min)
5	0.0323x + 0.8404	0.0323	0.9379		

10	0.0252x + 0.5459	0.0252	0.9736	2.1155	1.47×10^{-2}
25	0.0219x + 0.1968	0.0219	0.9991		
50	0.0183x + 0.0114	0.0183	0.9994		

To determine the mechanism of action of the UV light catalyzed by nano-Fe, a heterogeneous kinetic model based on a Langmuir-Hinshelwood (L-H) model was applied (Equation 6).

$$\frac{1}{k_{app}} = \frac{1}{k_c K_{LH}} + \frac{AB_o}{k_c} \tag{6}$$

Here, K_{LH} denotes the L-H adsorption equilibrium constant (L/mg) and k_c denotes the surface reaction rate constant (mg/L/min).

An R^2 value of the Langmuir-Hinshelwood kinetic plot (0.9173) indicated that the degradation of amido black dye conformed to the L–H model (Figure 7). The values of the L–H constants, i.e., K_{LH} and k_c, are presented in Table 1.
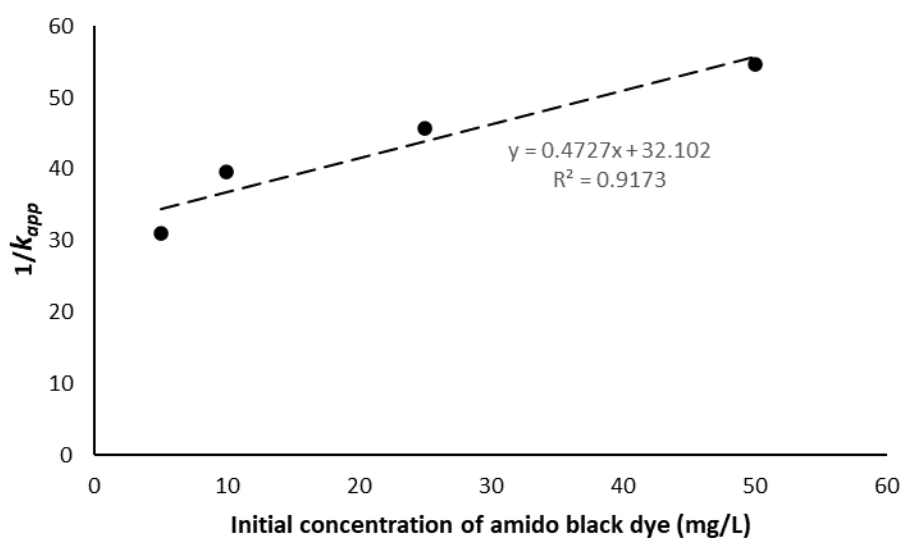

Figure 7 A Langmuir-Hinshelwood kinetic plot.

According to Akintayo et al. [22], photogenerated holes in the valence band h_{VB}^+ of the nano-Fe react with H_2O to form $OH^\bullet$. The e_{CB}^- in the conduction band generates electron resonance plasma over the catalyst surface (nano-Fe) and reacts with O_2 to produce $O_2^\bullet$. Thus, the $OH^\bullet$ and $O_2^\bullet$ radicals react with the amido black dye to form CO_2 and H_2O.

4. Conclusion

Wastewater treatment in the textile and dye industries involves the treatment of highly colored wastewater containing various dyes in different concentrations. The wastewater needs to be treated before discharge by effectively removing the dye color and other toxic compounds to protect the environment, following statutory guidelines. Thus, in this study, we showed that amido black dye can be removed by UV light catalyzed by nano-Fe. We found that the photocatalytic degradation of amido black dye by the nano-Fe/UV system strongly depended on the wavelength of the UV light, concentration of amido black dye, and the irradiation time. Moreover, higher

degradation of amido black dye by a combined nano-Fe/UV system might occur due to the synergistic interaction between UV light and nano-Fe. Therefore, the combination of UV light and nano-Fe catalysts might enhance the degradation of wastewater in the textile and dye industries. Further studies need to be conducted on the assessment of the toxicity of amido black dye after treatment, as well as, the identification of the intermediate species formed during degradation.

Author Contributions

OSA: Conceptualization, Supervision, Data curation, Writing – original draft, Writing – review and editing; CCO: Investigation, Data curation, Writing – original draft; OHA: Investigation, Data curation, Writing – original draft; OEO: Investigation, Data curation; OLO: Investigation, Data curation; COA: Supervision.

Competing Interests

The authors declared that no competing interests exist.

References

1. Khan N, Tabasi ZA, Liu J, Zhang BH, Zhao Y. Recent advances in functional materials for wastewater treatment: From materials to technological innovations. J Mar Sci Eng. 2022; 10: 534.
2. Patel H, Vashi RT. Removal of Congo red dye from its aqueous solution using natural coagulants. J Saudi Chem Soc. 2012; 16: 131-136.
3. Liu S, Ding Y, Li P, Diao K, Tan X, Lei F, et al. Adsorption of the anionic dye Congo red from aqueous solution onto natural zeolites modified with N,N-dimethyl dehydroabietylamine oxide. Chem Eng J. 2014; 248: 135-144.
4. Rahimi R, Kerdari H, Rabbani M, Shafiee M. Synthesis, characterization and adsorbing properties of hollow $Zn-Fe_2O_4$ nanospheres on removal of Congo red from aqueous solution. Desalination. 2011; 280: 412-418.
5. Ari AG, Celik S. Biosorption potential of Orange G dye by modified Pyracantha coccinea: Batch and dynamic flow system applications. Chem Eng J. 2013; 226: 263-270.
6. Peng L, Qin P, Lei M, Zeng Q, Song H, Yang J, et al. Modifying Fe_3O_4 nanoparticles with humic acid for removal of Rhodamine B in water. J Hazard Mater. 2012; 209-210: 193-198.
7. Kertèsz S, Cakl J, Jiránková H. Submerged hollow fiber microfiltration as a part of hybrid photocatalytic process for dye wastewater treatment. Desalination. 2014; 343: 106-112.
8. Khan TA, Dahiya S, Ali I. Use of kaolinite as adsorbent: Equilibrium, dynamics and thermodynamic studies on the adsorption of Rhodamine B from aqueous solution. Appl Clay Sci. 2012; 69: 58-66.
9. Adeyi O, Ayanda OS, Olutona GO, Ganiyu O. Adsorption kinetics and intraparticulate diffusivity of aniline blue dye onto activated plantain peels carbon. Chem Sci Trans. 2013; 2: 294-300.
10. Akolekar DB, Bhargava SK, Shirgoankar I, Prasad J. Catalytic wet oxidation: An environmental solution for organic pollutant removal from paper and pulp industrial waste liquor. Appl Catal A. 2002; 236: 255-262.

11. Ali I, Alharbi OML, Alothman ZA, Badjah AY. Kinetics, thermodynamics, and modeling of amido black dye photodegradation in water using Co/TiO_2 nanoparticles. Photochem Photobiol. 2018; 94: 935-941.

12. Ali I, Alharbi OML, Alothman ZA, Alwarthan A, Al-Mohaimeed AM. Preparation of a carboxymethylcellulose-iron composite for uptake of atorvastatin in water. Int J Biol Macromol. 2019; 132: 244-253.

13. Chen YH, Franzreb M, Lin RH, Chen LL, Chang CY, Yu YH, et al. Platinum-doped TiO_2/magnetic poly (methyl methacrylate) microspheres as a novel photocatalyst. Ind Eng Chem Res. 2009; 48: 7616-7623.

14. Xu P, Zeng GM, Huang DL, Feng CL, Hu S, Zhao MH, et al. Use of iron oxide nanomaterials in wastewater treatment: A review. Sci Total Environ. 2012; 424: 1-10.

15. Radini IA, Hasan N, Malik MA, Khan Z. Biosynthesis of iron nanoparticles using Trigonella foenum-graecum seed extract for photocatalytic methyl orange dye degradation and antibacterial applications. J Photochem Photobiol B. 2018; 183: 154-163.

16. Bishnoi S, Kumar A, Selvaraj R. Facile synthesis of magnetic iron oxide nanoparticles using inedible Cynometra ramiflora fruit extract waste and their photocatalytic degradation of methylene blue dye. Mater Res Bull. 2018; 97: 121-127.

17. Bibi I, Nazar N, Ata S, Sultan M, Ali A, Abbas A, et al. Green synthesis of iron oxide nanoparticles using pomegranate seeds extract and photocatalytic activity evaluation for the degradation of textile dye. J Mater Res Technol. 2019; 8: 6115-6124.

18. Meneceur S, Hemmami H, Bouafia A, Laouini SE, Tedjani ML, Berra D, et al. Photocatalytic activity of iron oxide nanoparticles synthesized by different plant extracts for the degradation of diazo dyes Evans blue and Congo red. Biomass Convers Biorefin. 2022. doi: 10.1007/s13399-022-02734-4.

19. Mithun Prakash R, Ningaraju C, Gayathri K, Teja YN, Aslam Manthrammel M, Shkir M, et al. One-step solution auto-combustion process for the rapid synthesis of crystalline phase iron oxide nanoparticles with improved magnetic and photocatalytic properties. Adv Powder Technol. 2022; 33: 103435.

20. Ayanda OS, Nelana SM, Naidoo EB. Ultrasonic degradation of aqueous phenolsulfonphthalein (PSP) in the presence of nano-Fe/H_2O_2. Ultrason Sonochem. 2018; 47: 29-35.

21. Alegbe MJ, Ayanda OS, Ndungu P, Nechaev A, Fatoba OO, Petrik LF. Physicochemical characteristics of acid mine drainage, simultaneous remediation and use as feedstock for value added products. J Environ Chem Eng. 2019; 7: 103097.

22. Akintayo CO, Aremu OH, Igboama WN, Nelana SM, Ayanda OS. Performance evaluation of ultra-violet light and iron oxide nanoparticles for the treatment of synthetic petroleum wastewater: Kinetics of COD removal. Materials (Basel). 2021; 14: 5012.
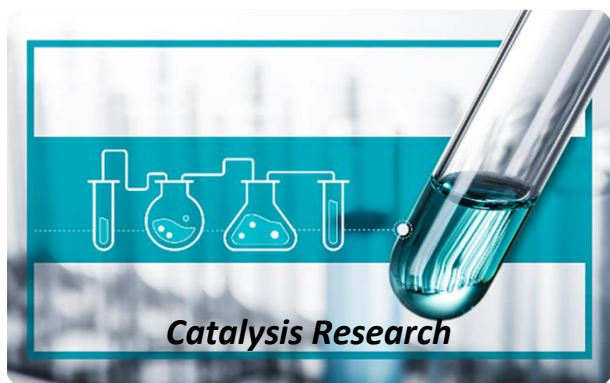
Enjoy *Catalysis Research* by:

1. [Submitting a manuscript](#)
2. [Joining in volunteer reviewer bank](#)
3. [Joining Editorial Board](#)
4. [Guest editing a special issue](#)

For more details, please visit:
http://www.lidsen.com/journals/cr